The Use of Remote Sensing in Estimating Irrigated Land In New Mexico

Report for Interstate Stream Commission

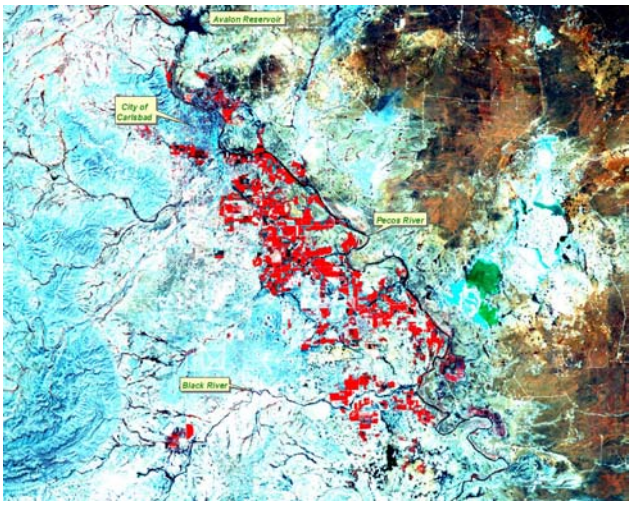

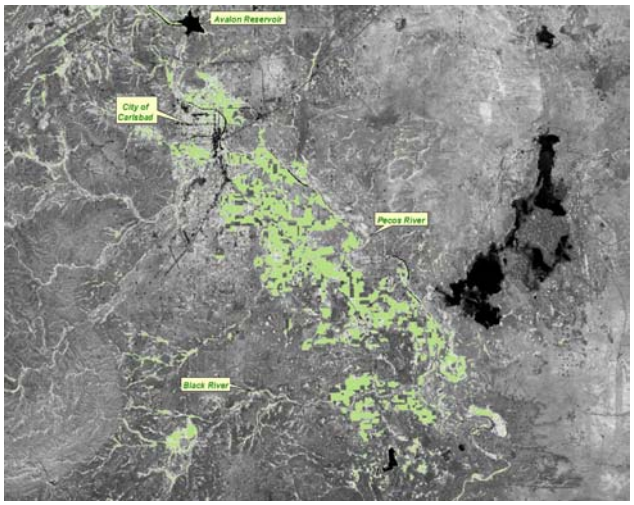

By

Dario Rodriguez
Nabil Shafike

September 2004

AGRICULTURAL LAND MONITORING PROGRAM IN NEW MEXICO

INTRODUCTION

The mission of the New Mexico Office of the State Engineer and the Interstate Stream Commission (OSE/ISC) is to develop, protect, conserve, and manage the state's finite water resource. The OSE/ISC must administer New Mexico's water to meet the needs of existing appropriations and users, comply with all interstate river compact obligations, and protect the state's waters from unauthorized use. However, administration of the state's water supply to meet existing and future uses involves working within a natural system with attendant and complex uncertainties that present considerable management challenges. As a prior-appropriation state, New Mexico must administer to protect senior water rights owners. However, as New Mexico grows, there are ever increasing demands from more junior users; clearly, effective and efficient water management technologies are required.

The Office of the State Engineer and the Interstate Stream Commission (OSE/ISC) have put in place an "Active Water Resource Management" strategy designed to protect, manage and develop New Mexico's water resources. This strategy encompasses three main elements: measurement, management and marketing. Measuring means an accurate determination of water supply and water use. Management means the efficient and effective use of surface and groundwater. Marketing entails development of water markets to meet water use demands. All these elements are framed within the state's prior appropriation doctrine and the water rights established under that doctrine.

Up-to-date and innovative technologies are always being sought to establish accurate and timely measurements that form the foundation of any active water management strategy. This report illustrates the use of satellite imagery and remote sensing technology to develop an inventory of irrigated and riparian acreages as a first step to develop an annual water depletion model of the state. The following sections describe the methodology and its application to a pilot area on the lower Pecos River Basin. Finally the technique was applies to a larger area in the Lower Rio Grande (from Caballo Dam to the State line).

METHODOLOGY

The agriculture land monitoring program (ALMP) main objective is to develop and implement a methodology that will allow the quantification of agricultural cropped areas and seasonal patterns of agricultural water uses along major river basins in the state of New Mexico. A secondary objective is to develop a computer-based system (software and hardware) to analyze remotely sensed data and overlay the results on a geo-referenced base.

The remotely sensed data consist of Landsat ETM$^+$ multi-spectral satellite imagery, whose general characteristics are shown in the table below.

Table 1 - Landsat ETM$^+$ bands, resolutions, and spectral ranges (USGS, 2003).

Band	Spatial Resolution	Wavelength (microns)	Spectral Location
1	30m (98 ft)	0.45-0.52	Blue visible
2	30m (98 ft)	0.52-0.60	Green visible
3	30m (98 ft)	0.63-0.69	Red visible
4	30m (98 ft)	0.76-0.90	Near-infrared
5	30m (98 ft)	1.55-1.75	Mid-infrared
6	60m (197 ft)	10.4-12.5	Thermal Infrared
7	30m (98 ft)	2.08-2.35	Mid-infrared
8	15m (49 ft)	0.52-0.90	Panchromatic

Landsat ETM$^+$ can resolve a field as small as 0.22 acres in the 1 thru 5 and 7 bands, while band 6 (thermal band) can only resolve a field as large as 0.89 acres. On the other hand, the single panchromatic band 8 can resolve a field as small as 0.06 acres.

The methodology consists of three fundamental steps:

- Acquire cloud-free satellite imagery at three different times of the growing season (spring, summer and fall);
- Analyze that imagery digitally using a vegetation index such as the Normalized Difference Vegetation Index (NDVI) to determine irrigated lands throughout the state; and
- Compare the results to existing databases.

After geometric and radiometric corrections of the image, an NDVI value for each image and time is developed to illustrate the healthy vegetation at that place and time. NDVI is defined as the normalized difference between the near-infra red and the visible red bands of the Landsat ETM$^+$ (i.e. [Band 4-Band 3] / [Band 4+Band 3]*100). Then the three NDVI images are combined as shown in the schematic below to generate one image representing the healthy vegetation during the growing season. Each NDVI is then assigned to a unique number: 1 for April 12, 3 for July 17, and 5 for Sept. 19. All three images are then added together into a single file with unique numbers for all date combinations resulting. The diagram below shows the possible image date combinations with their unique numbers shown in red. Each pixel of the final image has an attribute that indicates the activity on this pixel. For example one pixel may be irrigated during one time only, or during two or three times.

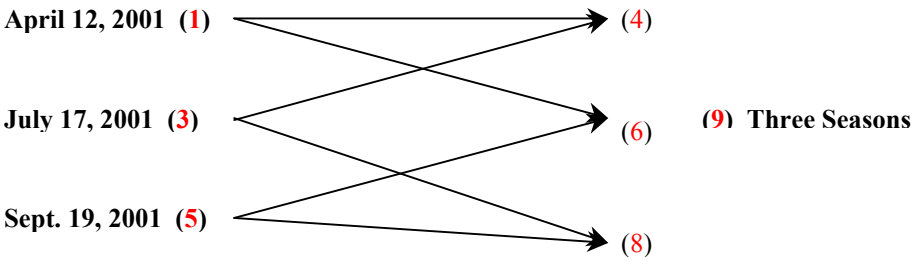

Figure 1 – NDVI Diagram.

PILOT STUDY

The above methodology was tested using a pilot study area located in the southern portion of the Pecos river basin and included portion of north east Texas as shown in figure below. The 2001 satellite imagery was used and the results were compared to the hydrographic survey data produced by OSE/ISC.

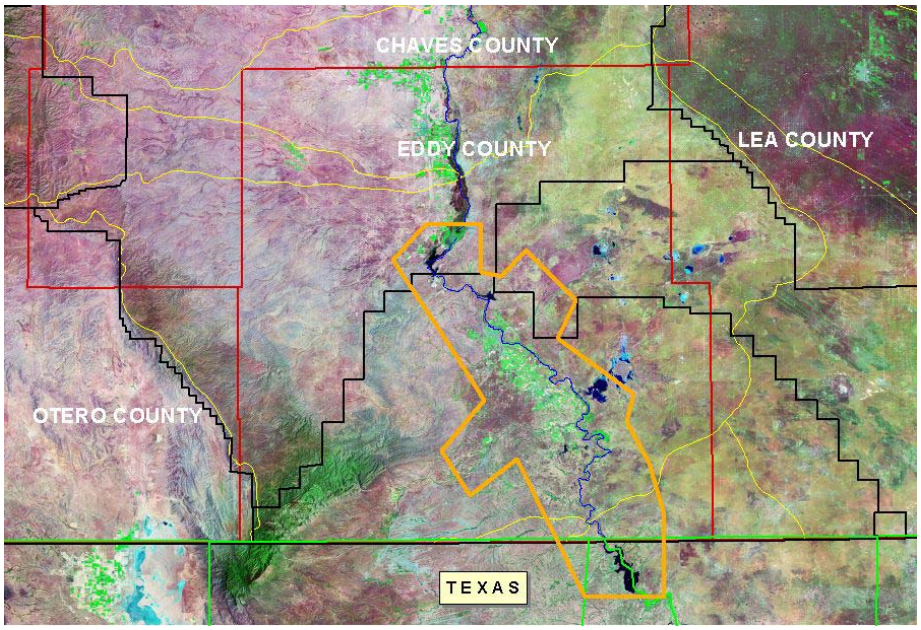

Figure 2 – Pilot Area.

The pilot area included the Carlsbad Underground Basin (CUB) and the Carlsbad Irrigation District (CID). The OSE Hydrographic Survey Bureau (HSB) conducted a hydrographic survey of the CUB and CID in 2000-2003. Digital orthophotography from 2001 aerial photography was produced, and preliminary mapping of individual tracts were available for the analysis

Considering historical data availability, spectral characteristics and cost, the Landsat ETM$^+$ system was selected for this initial phase. A single Landsat image covers the pilot area completely. However a complete coverage of the Rio Grande and the Pecos River corridors would require nine images (See figure below). The dates of available Landsat satellite imagery selected for this analysis were April 12, July 17 and September 19, 2001.

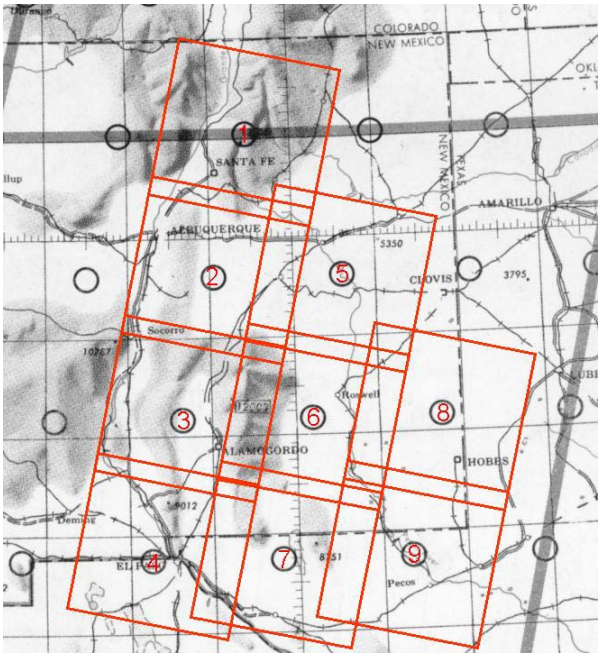

Figure 3 – Image Coverage of Pilot Area.

The determination of green, healthy vegetation was obtained using a normalized difference vegetation index (NDVI), calculated from visible and reflected infrared portions of light (Spectral bands 3 an 4 of Landsat ETM$^+$). This spectral analysis has been found to be adequate to determine vegetated versus non-vegetated areas. The visible and infrared bands or channels of data represent reflected light intensity values from the landscape. A more detailed description of the satellite imagery and digital analysis utilized is presented in Appendix A: Image Analysis.

RESULTS OF PILOT STUDY

An NDVI for each of the three selected images were derived. These estimates were obtained such that each pixel or green, healthy vegetation unit were counted only once.

Then, the estimates were aggregated to determine a total green, healthy vegetation area. The figure on the right below shows one of the Landsat images used (12April01) in a color combination that highlights green, healthy vegetation in bright red and several landmarks. The figure on the left represents the resulting NDVI image.

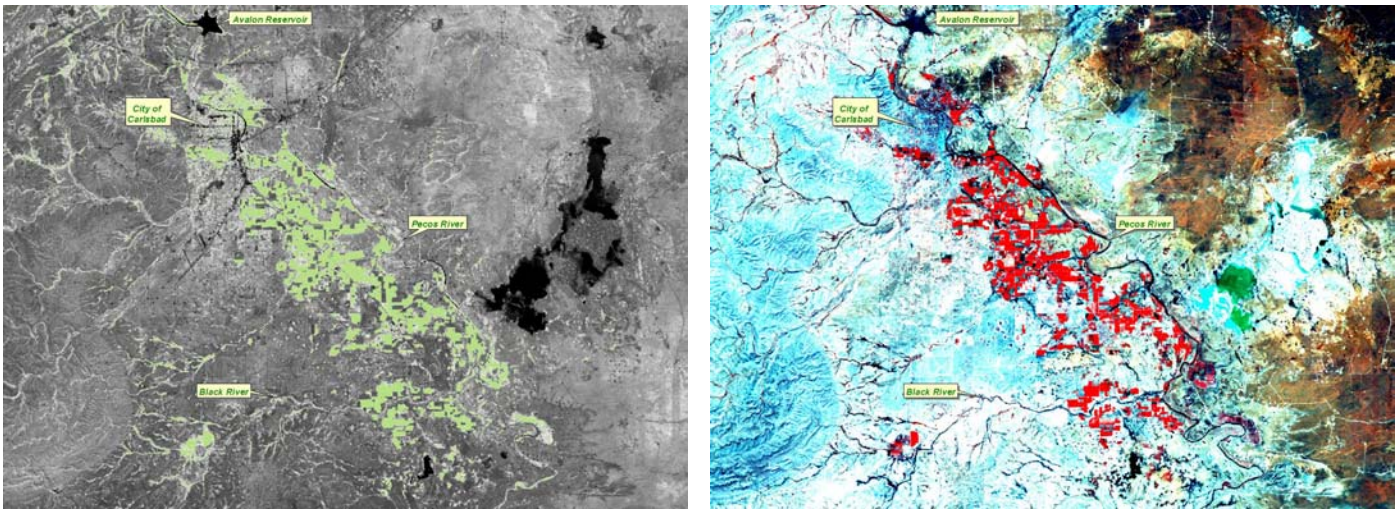

Figure 4 – NDVI Preliminary Results in the Pilot Area.

The final NDVI result, the three dates combined, was compared visually to the orthophoto base produced by Hydrographic Survey Bureau in July 2001. The water use map layers produced by HSB are shown below for the CID, CUB and Black River areas and for Townships 23S and 24S (There was no coverage for Township 22S, and a gap can be seen.). The visual comparison between the NDVI coverage and the HSB map layers showed a remarkable similarity, which was reflected in the numerical analysis of areas identified by the NDVI and the map layers.

The figure below shows the HSB map layers, where the similarity between this HSB combined map and the NDVI results seem apparent.

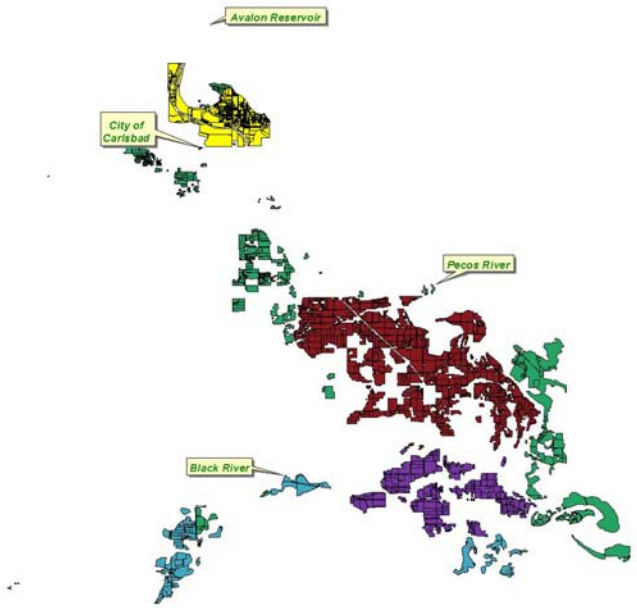

Figure 5 – NDVI Combined Results in the Pilot Area.

The table below presents the results of the NDVI analysis for CID, CUB and Black River areas

Table 2 – NDVI Preliminary Results in the Pilot Area.

Date Combination	Acreage
April 12, 2001 only	1,588.1
July 17, 2001 only	2,392.5
April 12 and July 17 only	2,707.9
Sept. 19, 2001 only	633.8
April 12 and Sept. 19 only	590.7
July 17 and Sept. 19 only	2,471.0
All dates present only	4,120.3
Total	***14,504.4***

As mentioned above, these results include several townships for which HSB data did not exist at the time. If we compare the existing HSB data for Townships 23S and 24S, the total irrigated area, excluding formerly irrigated areas, is 15,231 acres.

AGRICULTURAL LAND MONITORING

The methodology applied in the Pilot Study and the results for 2001 were the basis for undertaken an analysis of agricultural lands statewide. Satellite and HSB data were acquired and compiled to determine agricultural crop lands in New Mexico using an unsupervised classification based on NDVI analysis.

The satellite data were obtained for three different dates: early-mid spring, early-mid summer, and early fall. These dates coincide with the agricultural crop growth patterns of the study area. The remotely sensed data collected covered the beginning of the growing season in the spring (mid-April), the mature stage in the summer (July), and at senescence in the fall (September). The table below shows the images used.

Table 3 – Images used in this project identified in *pprrmmddyyyy* format, where *pp* is path, *rr* is row, *mm* is month, *dd* is day, and *yyyy* is year (i.e. Path 31 Row 37, April 15, 2002).

Spring	Summer	Fall
313704152002	313706182002	313709222002
313804152002	313806182002	313809222002
323604222002	323606252002	323610152002
323704222002	323706252002	323710152002
323803212002	323806252002	323810152002
343504042002	333507182002	333509202002
343604042002	333607022002	333609202002
343704042002	333707022002	333709202002
333803122002	333807022002	333809202002

The state coverage of these images is shown in the figure below. Notice that the summer and fall area coverage is the same (identical Path/Row but different dates).

Figure 6 - Outlines of images used for spring (left), summer and fall (right).

Several spatial and spectral processes are applied to the data before the digital analysis takes place. The former process consisted of a rectification of the images to a map base, and the latter consisted of a radiometric correction of the data. The rectification defines the projection and coordinate system and allows measurements of area to be performed. The radiometric correction removes systematic signal distortion of the sensor.

With the images rectified and radiometrically corrected a digital analysis is possible. This analysis takes advantage of the spectral characteristics of two bands, 3 and 4. Band 3 detects the absorption of solar radiation by active chlorophyll of green vegetation, and band 4 detects the reflectance of chlorophyll. The ratio of the difference of these two bands has been found to correlate with the presence of green, healthy vegetation.

The HSB data compiled were shapefiles and irrigated tracts from hydrographic surveys conducted by OSE. A particular coverage called the Water Use Monitoring and Planning (WUMAP) map produced by OSE was initially used to restrict the digital analysis to a buffer area surrounding main river areas. This WUMAP shapefile was further refined to cover only those areas were agriculture water use was known to take place. Further still, the validation of the methodology was done using shapefiles of the Nutt-Hockett and Lower Rio Grande areas where hydrographic surveys had been conducted in 1997-2001. These surveys provided the irrigated tract acreage used to compare digital analysis results.

RESULTS

An NDVI digital analysis of the satellite imagery for 2002 was conducted. This digital analysis of these multi-spectral satellite data detected areas covered by green, healthy vegetation likely to be the product of agricultural practices, and areas presenting a natural vegetative cover. The former areas are considered agricultural lands, and the latter riparian and natural vegetation lands. The agricultural land acreage is the one reported and compared in this report.

The NDVI results were overlaid with the WUMAP. This is shown in the figure below.

It appeared that the NDVI results using the WUMAP coverage overstated potential agricultural lands by identifying forested areas as cropland. This is evident in the northeastern area of the state.

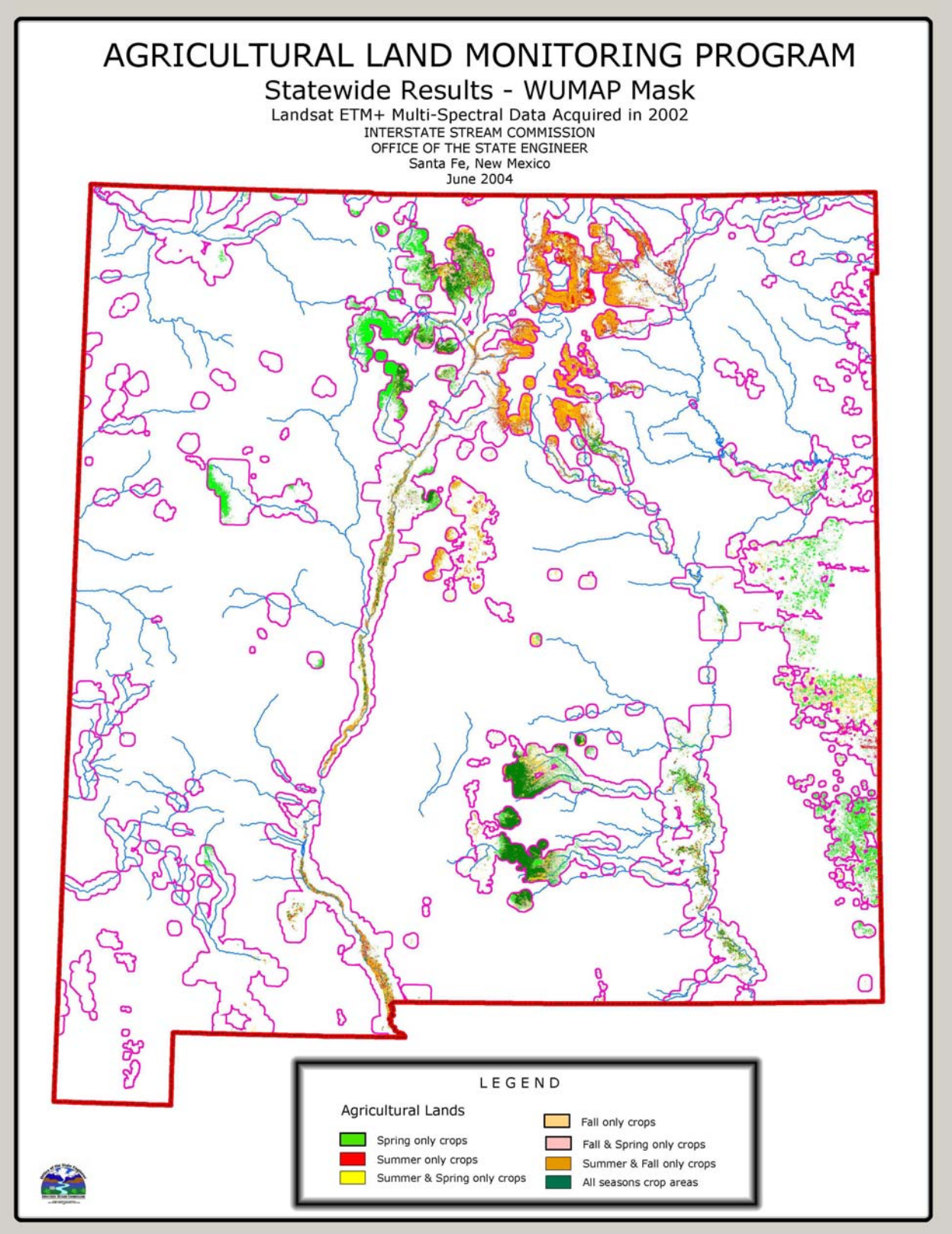

Figure 7 – NDVI results and WUMAP shapefile.

To reduce this problem a fine-tuned shapefile was produced containing only those areas that a visual inspection of New Mexico Bureau of Mines and Mineral Resources' Landsat Thematic Map of New Mexico would indicate having agricultural cropland. The NDVI results were overlaid with this fine-tuned coverage as shown below.

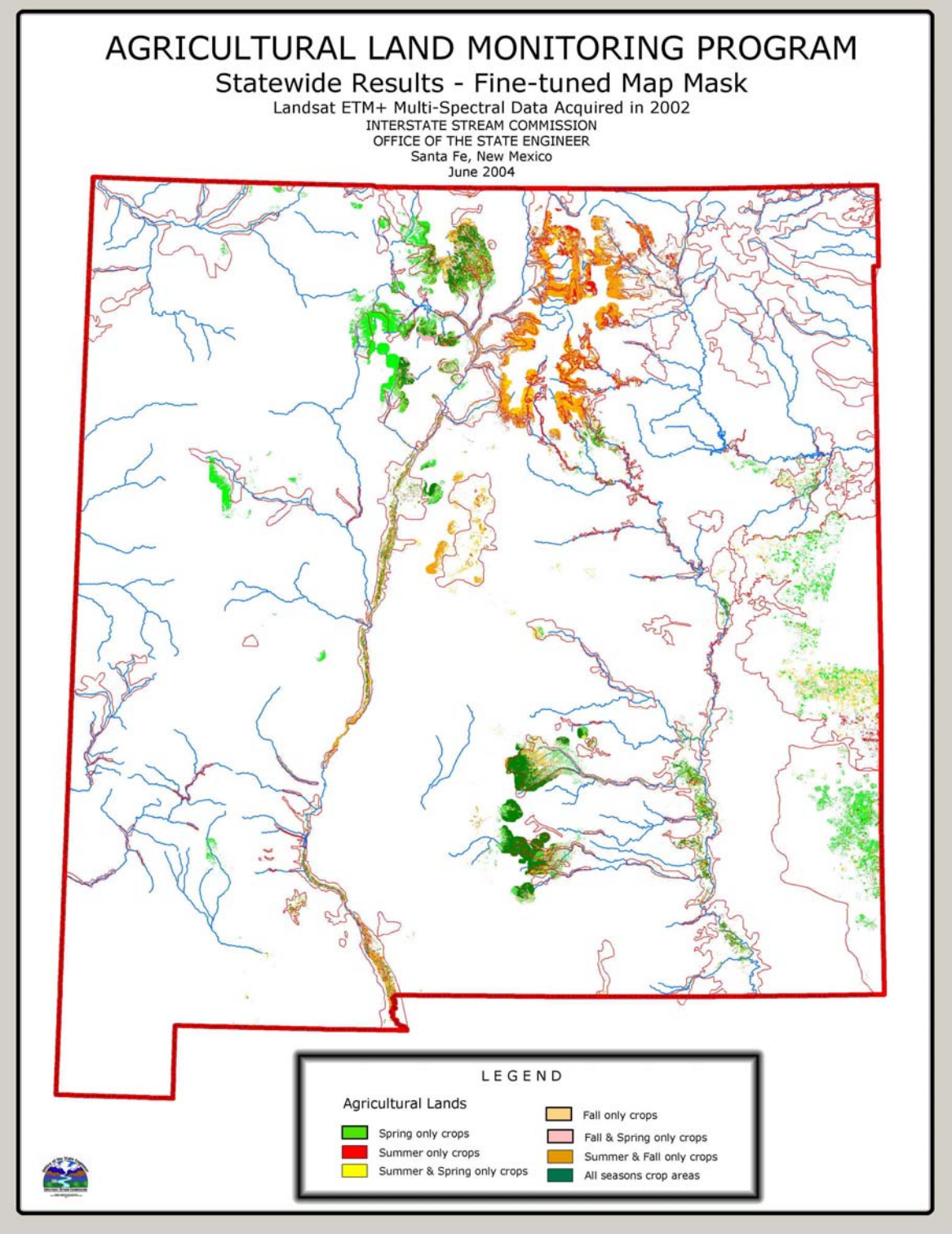

Figure 8 – NDVI results and fine-tuned coverage.

The fine-tuned map coverage subdivided the state into nine subareas: Canadian Eastern, Cimarron North East, Estancia, Gila-San Francisco, Pecos, Rio Grande, Salt Basin, San Juan, and Other Areas. This particular subdivision allowed the specific comparison between known hydrographic survey areas such as the Lower Rio Grande (LRG) and Nutt-Hockett Basins, and the Carlsbad Basin (CB) area.

Lower Rio Grande and Nutt-Hockett Basins

The LRG was extracted from the Rio Grande subarea and refined further to show the western, eastern and North Las Cruces parts of the LRG from Caballo Dam to the border with Texas. The NDVI results of these three parts, as well as the corridor along the Rio Grande, were then clipped from the statewide NDVI result and the areas calculated. The HSB office in Las Cruces has obtained over the years a very good estimate of agricultural area for the LRG, and these estimates are shown in the table below, together with the estimate for the Nutt-Hockett Basin. These numbers are paired with the NDVI estimates.

Table 4 – HSB cropland acreage and NDVI acreage results for 2002.

Area	HSB Acreage	NDVI Acreage
Nutt-Hockett	11,554	10,971
LRG*	99,182	95,888**
Totals	110,736	106,859

* LRG is subdivided into Rincon, Northern Mesilla, Southern Mesilla and Outside Areas. The total of these subdivisions is reported here.
** This total does not include Formerly Irrigated areas, estimated at 3% of the total.

These figures are all within 5% of each other, suggesting a high accuracy of the NDVI analysis.

For comparison purposes, two images of the Nutt-Hockett area NDVI and Landsat data were created and are shown below. The Landsat image is a False Color Composite (FCC) created using 1995-1998 imagery. The FCC shows agricultural crop vegetation as vivid green, and recently cropped areas as pinkish-blue.

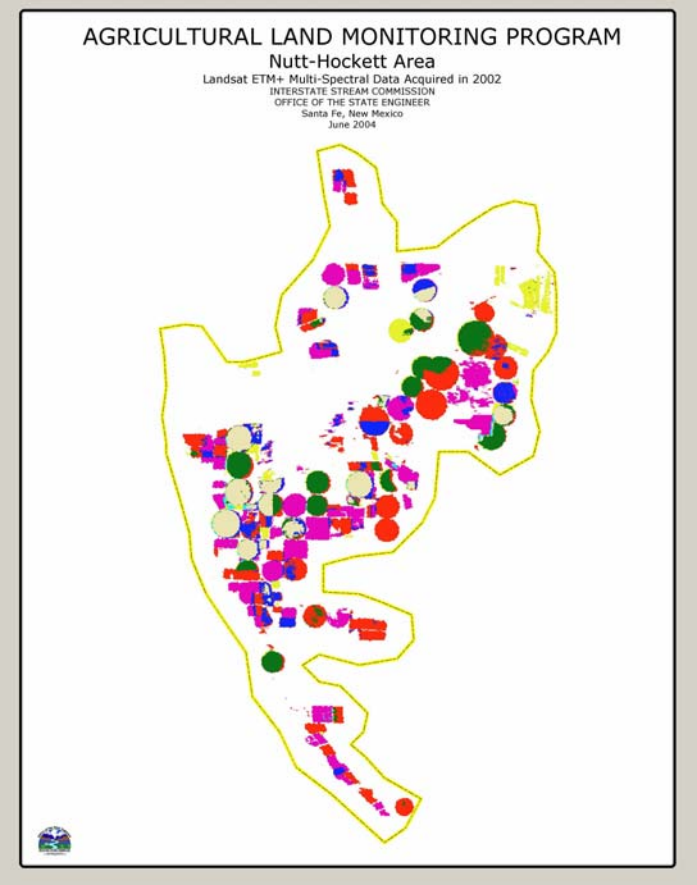

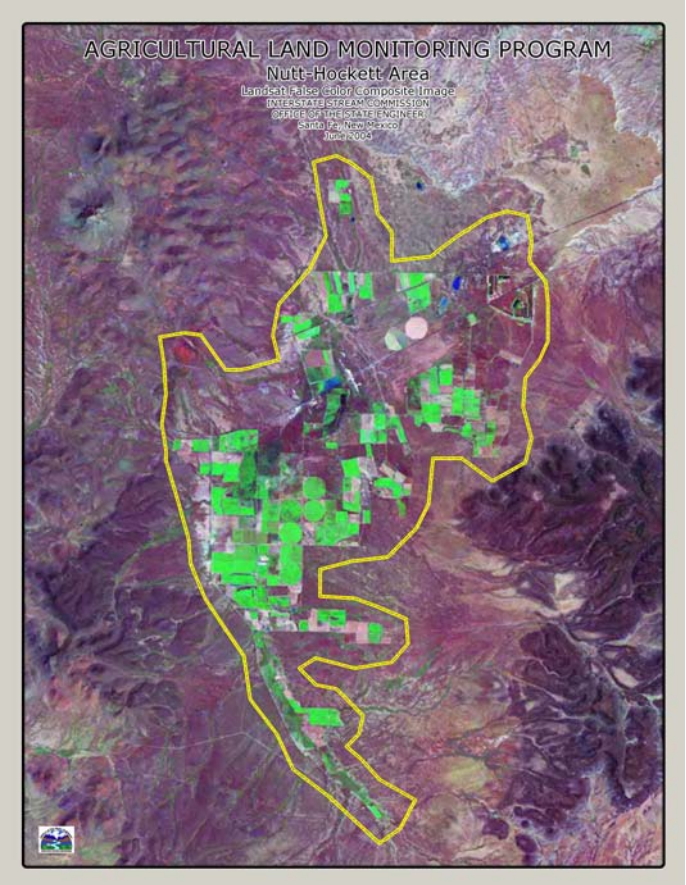

Figure 9 – Nutt-Hockett Aea NDVI results and Landsat FCC.

APPENDIX A: IMAGE ANALYSIS

Data Sources

Satellite Imagery

Landsat ETM$^+$ satellite imagery was chosen for this project to map the irrigated fields within the study area due to a number of advantages offered by this data type. The satellite imagery is acquired from a stable sensor platform and therefore is relatively easy to geometrically correct to a base map. The height of the sensor above the earth (approximately 440 miles) also negates most parallax problems commonly found in aerial photography (parallax is the apparent change in positions of stationary objects affected by the viewing angle – creating greater distortions at greater distances from the center of an aerial photo). The Landsat satellite platform acquires imagery along a roughly north-south orbital axis (path) recording data along an approximately 115 mile wide swath from west to east; this provides the large area coverage needed for a regional study such as this. In addition, it revisits this path every sixteen days, which facilitates the multi-temporal nature of this study. From a cost analysis basis, Landsat data has advantages over the other higher spatial resolution data vendors as it costs only pennies a square mile and the buyer can choose the imagery that best meets the study requirements. With the other commercially available imagery the data can cost up to tens of dollars a square mile and except for stipulations such as 20% maximum acceptable cloud cover the buyer gets the imagery acquired for the order even if it may be less than optimal for the study.

The principal disadvantage of the Landsat data is its spatial resolution, which is unable to resolve anything smaller than approximately 100 ft x 100 ft (0.2 acres). This is not necessarily a problem as large, pivot-irrigated fields are not only resolvable by the sensor but also easily interpretable on a computer monitor. However, smaller fields, especially when interspersed in a complex rural, riparian, urban matrix, are much harder to distinguish from the surroundings. Where this was would be a problem, GIS data sources such a field boundaries were expected to help mask out the response from the other vegetative classes from the irrigated fields.

The quantitative spectral aspects of ETM$^+$ imagery add particularly important dimensions to the mapping process. Multi-spectral satellite imagery records the variable reflection of natural radiation of surface materials such as rocks, plants, soils, and water. Landsat ETM$^+$, with six spectral bands at 30 meter resolution, one thermal band at 60 meters, and a panchromatic band at 15 meters, has the highest spectral discrimination among commercially available space-based sensors (Table 1).

Table 1 - Landsat ETM$^+$ bands, resolutions, and spectral ranges (USGS, 2003).

Band	Spatial Resolution	Wavelength (microns)	Spectral Location
1	30m (98 ft)	0.45-0.52	Blue visible
2	30m (98 ft)	0.52-0.60	Green visible
3	30m (98 ft)	0.63-0.69	Red visible
4	30m (98 ft)	0.76-0.90	Near-infrared
5	30m (98 ft)	1.55-1.75	Mid-infrared
6	60m (197 ft)	10.4-12.5	Thermal Infrared
7	30m (98 ft)	2.08-2.35	Mid-infrared
8	15m (49 ft)	0.52-0.90	Panchromatic

As useful as these other bands are for different types of mapping projects, only two bands were considered important for this particular study, specifically ETM$^+$ bands 3 and 4. These two bands emphasize reflectance response features that are unique to green vegetation compared to other major surface features such as dry vegetation and barren soil; namely band 3 maps the absorption of incoming solar radiation by active chlorophyll and band 4 maps an equally strong reflectance (Figure 1). Nonetheless, as a part of this project, all reflectance bands were processed so they would be ready for other potential uses.

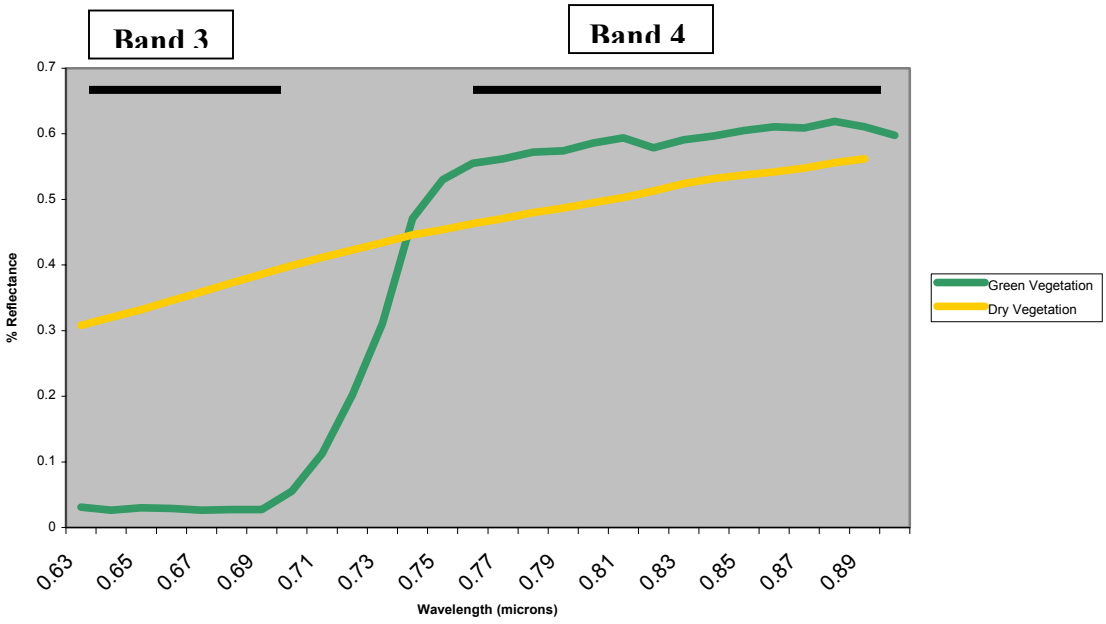

Figure 1 – Generic surface reflectance patterns of green vegetation vs. dry vegetation - soil response is similar to dry vegetation (derived from Bowker, *et al*., 1985).

The ETM$^+$ scenes used in this project were chosen so that irrigated fields in the Rio Grande and Pecos river basins were covered with imagery for spring, summer and

fall. After that, the guiding criteria were that each image be of good quality, with no clouds, cirrus or scan line defects, at least, over the irrigated fields. Even with its sixteen-day repeat visit cycle, it was still difficult to find cloudless imagery given the large regional scope of this project. Due to these problems, for the Rio Grande Basin, a different orbital path had to be chosen for the spring images versus the summer and fall images. In two other cases, a specific scene had to be acquired from a slightly different date than the other scenes along its path due to too much cloud cover. The images used are listed in Table 2 and the outlines of the area covered by the spring, summer and fall scenes are shown in Figure 2.

Table 2 – Images used in this project (identified in *pprrmmddyyyy* format, where *pp* is path, *rr* is row, *m* is month, *dd* is day, and *yyyy* is year).

Spring	Summer	Fall
313704152002	313706182002	313709222002
313804152002	313806182002	313809222002
323604222002	323606252002	323610152002
323704222002	323706252002	323710152002
323803212002	323806252002	323810152002
343504042002	333507182002	333509202002
343604042002	333607022002	333609202002
343704042002	333707022002	333709202002
333803122002	333807022002	333809202002

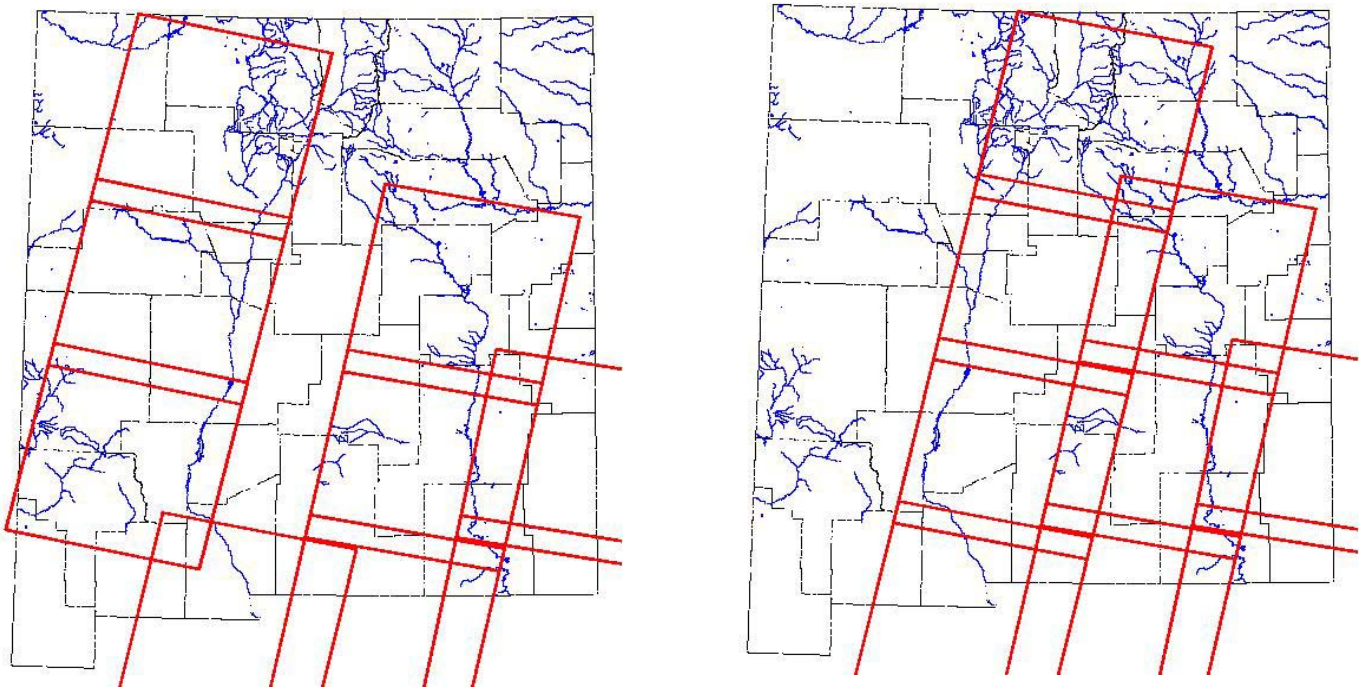

Figure 2 - Outlines of images used for spring (left), summer and fall (right).

Software Used

ERDAS IMAGINE, Version 8.5, was the principal software used throughout the mapping process. All digital imagery and GIS coverages were processed, manipulated, and used as overlays for analysis within the IMAGINE environment. ARC/GIS, Version 8.2, and ArcView 3.2 were used to create, import, and manipulate vector coverages.

Image Processing

Geometric Correction

The ETM^+ scenes were rectified to a map-based coordinate system using a nearest-neighbor interpolation. This process makes the image planimetric so that area, direction, and distance measurements can be performed. The image-to-map rectification process involves selecting a point on the map with its coordinate and the same point on the image with its x and y coordinate. The root mean square error (RMS_{error}) is computed to determine how well the map and image coordinates fit in a least-squares regression equation. The images were projected into the Universal Transverse Mercator, Zone 13, using the 1983 North American Datum and the 1980 Geodetic Reference System.

Reflectance Correction

A radiometric correction was performed on all ETM+ bands to account for the systematic signal distortion of the sensor. One major source of distortion that occurs is the sensor offset, the residual "black noise" that is recorded by the sensor when there is no input signal (Lillesand and Kiefer, 2000). The other major distortion is from the channel gain, which is the slope transfer relation between the signal received and the sensor's response. Differential offsets and gains between bands will cause problems when comparing their responses to a certain feature, so it is necessary to calibrate each band, especially in this case when it is important that features with the same reflectance from different areas and dates have the same image values. Gain and offset coefficients for each band are provided for in the image header. The effects of these deviations on the original data are modeled by Equation 1.

$$L = (DN*Gain) + Offset \quad \text{(Eq. 1)}$$

Where **L** is the output radiance value and **DN** is the input digital number value. The gain and offset coefficients for each of the scenes are given in Table 3 through 7.

Table 3 – Gain and offset coefficients for 313704152002, 313804152002, 323604222002, 323704222002, 323804222002, 343504042002, 343604042002, and 343704042002.

	Band 1	Band 2	Band 3	Band 4	Band 5	Band 7
Gain	0.77874	0.79882	0.62165	0.96929	0.12622	0.0439
Offset	-6.9787	-7.1988	-5.6217	-6.0693	-1.1262	-0.3939

Table 4 – Gain and offset coefficients for 313706182002, 323606252002, 323706252002, and 323806252002.

	Band 1	Band 2	Band 3	Band 4	Band 5	Band 7
Gain	0.77568	0.79568	0.61922	0.96549	0.12572	0.0437
Offset	-6.1999	-6.3999	-5	-5.1	-0.9999	-0.35

Table 5 – Gain and offset coefficients for 333803122002.

	Band 1	Band 2	Band 3	Band 4	Band 5	Band 7
Gain	1.18071	1.20984	0.94251	0.96929	0.19122	0.00664
Offset	-7.3807	-7.6098	-5.9425	-6.0693	-1.1912	-0.4165

Table 6 – Gain and offset coefficients for 333507182002, 333607022002, 333707022002, 333807022002, 333509202002, 333609202002, 333709202002 ,and 333809202002.

	Band 1	Band 2	Band 3	Band 4	Band 5	Band 7
Gain	1.17608	1.2051	0.93882	0.96549	0.19047	0.66235
Offset	-6.2	-6.3999	-5	-5.1	-1	-0.35

Table 7 – Gain and offset coefficients for 313709222002, 313809222002, 323610152002, 323710152002, and 323810152002.

	Band 1	Band 2	Band 3	Band 4	Band 5	Band 7
Gain	0.77568	0.79568	0.61922	0.96549	0.12573	0.04372
Offset	-6.1999	-6.3999	-5	-5.1	-0.9999	-0.35

Differences in incoming radiation due to the amount of the solar power spectrum distributed for each of the bandwidths can also cause differences in each band's response. These values, known either as solar irradiance or global solar constant, $\mathbf{G_{sc}}$, have been measured for each bandwidth and published by the Landsat mission group (Table 8).

Table 8 – Solar irradiance values for Landsat ETM+ bands in $mW/cm^2/\mu m$ (USGS, 2003).

	Band 1	Band 2	Band 3	Band 4	Band 5	Band 7
G_{sc}	1969	1840	1551	1044	225.7	82.069

Differences in the amount of incoming radiation due to the time of year as the distance between the Earth and the sun changes are also important. The relative inverse distance can be calculated in astronomical units (an unit measure equivalent to the average Earth-sun distance) using Equation 2.

$$d_r = 1 + 0.033\cos(DOY*(2\pi /365)) \quad \text{(Eq. 2)}$$

Where $\mathbf{d_r}$ is the inverse Earth-sun distance and **DOY** is the Julian day when the imagery was acquired.

Additionally, although the satellite acquires the imagery at the same solar time (approximately 10:30), the angle of sun when the imagery was acquired in relation to the sensor can vary with the time of year and can cause differences in the amount of illumination on the surface. This angle, known as the solar zenith angle, **θ**, can be calculated as the complement of the solar elevation angle, **SEA**, a value found in the header file for each image (Equation 3).

$$\theta = 90 - SEA \quad \text{(Eq. 3)}$$

Based on the image dates and the header file, the Earth-sun distance and solar zenith angles calculated for each image file are shown in Table 9.

Table 9 – The Julian day (DOY), Earth-sun distance (dr), solar zenith angle (θ) and its cosine for each image.

Scene ID	DOY	d_r	θ	cosθ
313704152002	105	0.991897	32.3	0.84526
313804152002	105	0.991897	31.6	0.85172
323604222002	122	0.982961	31.0	0.85716
323704222002	122	0.982961	30.3	0.86339
323803212002	80	1.006069	40.1	0.76492
343504042002	94	0.998102	37.7	0.79122
343604042002	94	0.998102	36.8	0.80073
343704042002	94	0.998102	36.0	0.80901
333803122002	71	1.011033	43.4	0.72657
313706182002	169	0.967753	23.7	0.91566
313806182002	169	0.967753	23.6	0.91636
323606252002	176	0.967142	24.3	0.91140
323706252002	176	0.967142	24.1	0.91283
323806252002	176	0.967142	23.9	0.91425
333507182002	199	0.968529	26.8	0.89258

Scene ID	DOY	d_r	θ	cosθ
333607022002	183	0.967013	23.5	0.91706
333707022002	183	0.967013	24.5	0.90996
333807022002	183	0.967013	24.4	0.91068
313709222002	265	0.995988	39.2	0.77494
313809222002	265	0.995988	38.2	0.78585
323610152002	288	1.009011	47.4	0.67687
323710152002	288	1.009011	46.2	0.69214
323810152002	288	1.009011	45.1	0.70587
333509202002	263	0.994856	40.6	0.75927
333609202002	263	0.994856	39.6	0.77051
333709202002	263	0.994856	35.9	0.81004
333809202002	263	0.994856	37.7	0.79122

These values then were used to model exo-atmospheric reflectance response values, **ρ**, for each image (Equation 4); these values accounts for changes due to both sensor perturbations and solar radiation differences, but do not address any differences due to atmospheric effects – those effects being much more difficult to model were not addressed in this project except through the initial image selection process by purposely choosing images that represented as close to clear sky conditions as possible.

$$\rho = (L*\pi) / (G_{sc}*\cos\theta*d_r) \text{ (Eq. 4)}$$

Normalized Difference Vegetation Index

A Normalized Difference Vegetation Index (NDVI) was created for each ETM^+ scene. The NDVI enhances the spectral surface response of vigorous vegetation shown in Figure1 by ratioing the chlorophyll reflection in band 4 over the absorption in band 3. The basic equation for the NDVI is shown in Equation 5 (ERDAS, 1999).

$$NDVI = (ETM^+4 - ETM^+3) / (ETM^+4 + ETM^+3) \text{ (Eq. 5)}$$

Where **ETM^+4** is the near infrared ETM+ band and **ETM^+3** is the visible red ETM+ band. The equation was further modified so as to get rid of negative values and to turn the data into integer values (thus decreasing disk space demand to one-quarter the size without sacrificing data content) using Equation 6:

$$NDVI_{(new)} = (1+NDVI) *100 \text{ (Eq. 6)}$$

Analysis

Each of the seasonal NDVI images was then mosaicked together. These mosaics were then analyzed over known irrigated fields to find the NDVI value which provided the best threshold separating the fields from surrounding vegetation. The values decided on are shown in Table 10.

Table 10 – NDVI Values used as thresholds for masking.

	Spring	Summer	Fall
Value	125	130	140

Every value above the threshold value was considered irrigated and changed to an output value of "1" and all values below the threshold were considered non-irrigated and changed to an output value of "0". The fact that the numbers are different and increase with each following season, may be in part be due to changes in the atmospheric effects on the different sets of imagery, but it is probably largely due to the need to increase the threshold value to provide better discrimination between the fields and the surrounding vegetation which due to late season green-up increasingly has values more similar to the irrigated fields.

Each of the thresholded seasonal mosaics were then reassigned such that wherever the spring image was "1" it remained a value of "1", wherever the summer image was "1" it was assigned a value of "3", and wherever the fall image was "1" it was assigned a value of "5". With these values reassigned, the seasonal mosaics were added together which resulted in a single image in which every possible combination of seasonal vegetative growth was assigned a unique value (Table 11) and avoided counting any pixel more than once.

Table 11 – Value assigned based on vegetative growth status.

Vegetative Growth Status	Value
No Vegetation	0
Spring Only	1
Summer Only	3
Fall Only	5
Spring and Summer Only	4
Summer and Fall Only	8
Spring and Fall Only	6
All Seasons	9

References

Bowker, D.E., R.E. Davis, D.L. Myrick, K. Stacy, and W.T. Jones, 1985. *Spectral Reflectances of Natural Targets for Use in Remote Sensing Studies*, NASA Reference Publication 1139, Hampton, Virginia.

ERDAS, 1999. *ERDAS Field Guide* (5th edition, revised and expanded). ERDAS, Inc., Atlanta, Georgia.

Lillesand, T.M. and R.W. Kiefer, 2000. *Remote Sensing and Image Interpretation*, 4th edition. John Wiley and Sons, Inc., New York.

USGS, 2003. Landsat Project website. Website, http://landsat7.usgs.gov, maintained by the U.S. Geological Survey, Reston, Virginia.